

## Study of the kinetic behaviour of non-enzymatic browning reaction between L-ascorbic acid and glycine by the excess concentration method

<sup>1</sup>\*Yang, Y., <sup>1</sup>Yu, A. N., <sup>2</sup>Sun, B. G., <sup>2</sup>Liu, Y. P. and <sup>2</sup>Tian, H. Y.

<sup>1</sup>School of Chemistry and Environmental Engineering, Hubei Minzu University, Enshi, 445000 Hubei Province, China

<sup>2</sup>Beijing Key Laboratory of Flavour Chemistry, Beijing Technology and Business University, Beijing, 100048, China

### Article history

Received: 5 September 2019

Received in revised form:

18 October 2019

Accepted:

7 November 2020

### Keywords

L-ascorbic acid,  
glycine,  
non-enzymatic browning  
reaction,  
kinetics

### Abstract

The formation kinetics of browning products (BPs) derived from the self-degradation of L-ascorbic acid (AA) and the reaction between AA and glycine (Gly) were investigated at pH 6.8 and various other parameters, such as temperature, time, and molar concentration ratio of AA/Gly. The temperature ranged from 110 to 150°C, the time ranged from 10 to 240 min, and the molar concentration ratios of AA to Gly were 4:1, 2:1, 1:1, 1:2, and 1:4. The results suggested that the formation rate of BPs was promoted by increasing the temperature, prolonging the time, and augmenting the molar ratio of AA. Based on the assumption of a kinetic model and a possible reaction pathway, the formation rate of BPs followed a pseudo-first order, and the rate was primarily dependent on the consumption of AA. The formation activation energies ( $E_a$ ) for the BPs were 60.76 and 70.16 kJ/mol with AA/Gly ratios of 4:1 and 1:4, respectively.

© All Rights Reserved

### Introduction

The non-enzymatic browning (NEB) reaction is a common reaction in the food industry (Stadler *et al.*, 2002; Kambo and Upadhyay, 2012), and mainly involves caramelisation, the Maillard reaction, and the degradation reaction of L-ascorbic acid (AA) (Vernin *et al.*, 1997; Mitra *et al.*, 2015). In food processing, NEB reactions generate an unpleasant and deleterious changes that negatively affect nutritional value. However, NEB reactions are desired in some food processes because their products characterise the final food that is obtained such as in caramel, candies, sweet milk, and in crusts produced during baking. The Maillard reaction is a reaction between amino acids/proteins and reducing saccharides (Maillard, 1912; Hodge, 1953; Martins *et al.*, 2000), and has a remarkable influence on food composition and properties. To generate browning product (BP) reactions, the degradation of AA should not be ignored. There are many reports on the degradation of AA (Tiwari *et al.*, 2009; Sapei and Hwa, 2014; Gabriel *et al.*, 2015) or the reaction between AA and amino acids. These two reactions take part in the formation of BPs (Shallenberger *et al.*, 1959; Rogacheva *et al.*, 1995; Yu *et al.*, 2012b; 2017). The NEB reaction is complex in nature, and involves a number of intermediate complexes (Martins and Boekel, 2005a; 2005b) such as un-colourful intermediate products (UIPs) and BPs

(Boekel, 1998; Benjakul *et al.*, 2005). Many studies have examined the influences of reaction parameters on the formation of BPs in the NEB reaction. It has been demonstrated that reaction parameters such as temperature, time, and surroundings have prominent effects on the formation of BPs (Mundt and Wedzicha, 2003). The kinetic behaviour of the NEB reaction between AA and L-glutamic acid or L-aspartic acid has been reported (Zhou *et al.*, 2016; Yu *et al.*, 2017). The most common method of expressing browning is to measure colour absorption as a function of time, and to express the reaction kinetics. Understanding the dynamics of the formation of BPs is the main focus for optimising the preservation process of fruits and vegetables, including juice and puree of fruits and vegetables (Montano *et al.*, 2006). The relationship between the absorbance at 420 nm and time has been studied in the NEB reaction. It has been found that the absorbance at 420 nm is a function of time, which would fit to different kinetic models such as zero- and first-order, Weibull, logistic, and parabolic models (Ahrné *et al.*, 2007; Isleroglu *et al.*, 2012). In the studies mentioned above, the dynamic model for the formation of BPs is mainly based on the basic equation of Arrhenius, from which the constant rate formation of BPs is obtained. Following the change in the absorbance at 420 nm during storage at a constant temperature (20 - 50°C), previous studies (Wedzicha and Mcweeny, 1974; Lertittikul *et al.*, 2007; Yu *et al.*,

\*Corresponding author.  
Email: [yanyang8069@163.com](mailto:yanyang8069@163.com)

2012b; Li *et al.*, 2016a) have shown that BPs are formed according to a pseudo-first order. However, a special kinetic model for BP formation has not been established. The measurement of reaction kinetics provides the most common way to determine its possible mechanism, and can help food scientists make decisions about how to optimise processes in the food industry.

In the present work, the kinetics of NEB development were investigated at pH 6.8, temperatures of 110 - 150°C, and times of 10 - 240 min, in a system containing various ratios of AA and Gly. The formation kinetics of BPs were studied by the method of complex reaction kinetics. The dynamic model of BP formation was proposed based on the approximate processing of complex reactions. The formation activation energy ( $E_a$ ) was calculated at different ratios of AA/Gly. In addition, the influences of reaction factors on the formation of precursors, UIPs, and BPs are also discussed.

## Materials and methods

### Reagents

All the experimental reagents such as L-ascorbic acid (AA), glycine (Gly), NaCl,  $\text{HPO}_3$ ,  $\text{NaH}_2\text{PO}_4$ ,  $\text{Na}_2\text{HPO}_4$ , NaOH, and 2,4-dinitrofluorobenzene were of AR grade. Other reagents such as methanol and acetonitrile were of HPLC grade. All of these were purchased from Sinopharm Chemical Reagent Co., Ltd. (Shanghai, China). Water was redistilled before use.

### Model reaction between AA and Gly

The concentrations of AA and Gly ranged from 0.035 to 0.140 M according to the requirements of different ratios of AA/Gly, which were 4:1, 2:1, 1:1, 1:2, and 1:4, as shown in Table 1. Different ratios of AA and Gly were dissolved in a buffer solution ( $\text{Na}_2\text{HPO}_4$ - $\text{NaH}_2\text{PO}_4$ , 0.2 M), and adjusted to pH 6.8 without air involved in the reaction bottle, which was displaced by nitrogen. In a previous study (Li *et al.*, 2016a; 2016b; 2016c), it was found that the microcosmic environment of the solution was not changed much, in that, the change in pH value of the solution was not particularly obvious when pH value of the solution was 6.8. Moreover, it was more conducive to the formation of BPs under these conditions. Therefore, these reaction parameters were chosen to study the NEB reaction of AA/Gly.

The mixtures were divided into three aliquots of 10 mL each. Each aliquot was sealed in a 15 mL Synthware pressure glass vial (Beijing Synthware Glass, Inc., China), and heated with stirring at

Table 1. Five reactants ratio of AA/Gly for NEB reaction.

Reaction system code	AA molarity (mmol)	Gly molarity (mmol)
4:1	1.400	0.350
2:1	0.700	0.350
1:1	0.350	0.350
1:2	0.350	0.700
1:4	0.350	1.400

different temperatures (110 - 150°C) for different time periods (10 - 240 min) in an oil bath.

The temperature was controlled through an Omega temperature controller ( $\pm 0.2^\circ\text{C}$ ) provided with a type "K" thermocouple (Li *et al.*, 2016b). The reaction was stopped by immersion of the sealed tubes in a water-ice bath when the desired reaction time had elapsed. Experimental errors were estimated by repeating the experiments in triplicate at minimum under identical experimental conditions, and each data point was collected from three samples. All solutions were prepared in double distilled water.

### Analytical methods

The concentrations of AA and Gly residues in solution were determined by reverse phase (RP) high-performance liquid chromatography (HPLC) (Agilent; Santa Clara, CA, USA), which was an Agilent Technologies model 1260 instrument, equipped with a UV diode array detector and a  $\text{C}_{18}$  (3.5  $\mu\text{m}$ , 4.6 mm i.d.  $\times$  100 mm) column. AA and Gly were quantified based on an external standard procedure using a calibration curve of AA and Gly standard samples ( $R^2 = 0.9998$ ), respectively.

Each data point was collected from three samples. All experiments were carried out in triplicate at minimum with a relative standard deviation (RSD) of less than 4.5%.

### Quantification of AA concentration

The detection conditions for AA were a mobile phase elution composed of 0.1 weight percent (wt. %) water/methanol/meta-phosphate in gradient elution mode (Tang *et al.*, 2014; Li *et al.*, 2016a). The standard curve of AA was  $y = 30.1076x + 6.6447$  (concentration of AA,  $\mu\text{g/mL}$ ;  $y$  = area of absorbance of AA; and  $R^2 = 0.9996$ ).

### Quantification of Gly concentration

Before detection, the production sample was derived by 2,4-dinitrofluorobenzene (FDNB) in

alkaline conditions, which was a solution of 1 mL NaHCO<sub>3</sub> (0.05 M). The FDNB solution, approximately 2 wt. %, was dissolved in 1 mL of acetonitrile. This solution was reacted in a water bath at 60°C for 60 min without light. Finally, the sample was cooled by immersion in a water-ice bath, and diluted to 10 mL with a buffer solution phosphate (0.01 M). The sample was filtered prior to detection. The mobile phase elution consisted of a water/acetonitrile/phosphate buffer solution (0.01 M) in a gradient elution mode (Zhou *et al.*, 2015). The flow rate was 1.0 mL/min, the column temperature was 30°C, the injection volume was 5 µL, and the detection wavelength was 360 nm. The standard curve of Gly was  $y = 5739.4264x - 39.1401$  (concentration of Gly, µg/mL;  $y$  = area of absorbance of Gly; and  $R^2 = 0.9991$ ).

#### Quantification of UIPs and BPs

The solution absorbance of the NEB reaction was measured according to previous works (Tang *et al.*, 2014; Li *et al.*, 2016a). During the NEB reactions, the solution, which came from the self-degradation products of AA and reaction products of AA/Gly, had a special absorption peak at 294 nm due to the conjugation effect of the products (Ajouz *et al.*, 2010). This value can be used to represent the process of accumulation of some small molecules, which can be used to characterise a series of products before the browning products were formed, namely the browning product precursor, also known as un-colourful intermediate products (UIPs).

According to reports in the literature (Benjakul *et al.*, 2005; Yu *et al.*, 2012a), when the absorbance of UIPs accumulate to a certain level, the final stage of the degradation products of AA and reaction products of AA/Gly is the occurrence of brown products, the solution colour changed, and the absorption could be measured at 420 nm. The absorbance of the system at 420 nm indicates the extent of the formation of macromolecular brown matter, namely, the browning products (BPs).

The UV-absorbance and browning intensity of the reaction solutions were measured at an ambient temperature of 294 nm (Benjakul *et al.*, 2005; Ajouz *et al.*, 2010; Yu *et al.*, 2012a; Zhou *et al.*, 2015) and 420 nm (Lerici *et al.*, 1990; Brands *et al.*, 2000) by using a Cary 300 spectrophotometer (Shimadzu Co., Ltd., Kyoto, Japan). If necessary, the product was diluted appropriately (25, -50, or -100 times) to obtain absorbance values no higher than 1.000, to ensure the values of absorbance of solution in the Lambert and Beer's range. The final results in the figures are presented with the dilution factor. All the experiments were carried out in triplicate. The average RSD was

less than 4.5% for each triplicate experimental result.

#### Kinetic modelling

The NEB reaction of self-degradation of AA and reaction of AA/Gly is very complex, which makes the kinetic description of NEB very difficult. The kinetic model for the formation of BPs was established during the NEB reaction, which came from the self-degradation of AA and the reaction of AA/Gly according to the steady-state approximation rule and the fast-step approximation methods (Bhore *et al.*, 1990; Leong and Wedzicha, 2000; Martins and Boekel, 2005b; Serpen and Gokmen, 2007).

The consumption rate of AA as a function of concentrations of AA and Gly can be expressed simply as a power-law rate (Eq. 1):

$$\frac{dC_{BP}}{dt} = kC_{AA}^{\alpha}C_{Gly}^{\beta} \quad (\text{Eq. 1})$$

where,  $k$  = rate constant, and  $\alpha$  and  $\beta$  = reaction orders for AA and Gly, respectively. Herein, the kinetics of the NEB reaction between AA and Gly are discussed by using the method of excessive concentration.

#### Statistical analysis

Data were acquired based on experimental results, which were carried out in triplicate at minimum while controlling the RSD within 4.5%. All data were processed using Microsoft Office 2010 and Origin 8.5.

## Results and discussion

#### Correlations between absorbance values of UIPs and BPs, and the concentration of AA/Gly

The correlations between the absorbance values of UIPs and BPs, the concentration of AA/Gly at 110 and 150°C, and various molar ratios of AA/Gly are shown in Figures 1 and 2. At both temperatures, the concentration of AA and Gly decreased, and the absorbance of UIPs and BPs increased with prolonged time. Comparing Figures 1 and 2, it was found that temperature had a remarkable effect on the consumption of AA/Gly and the formation of UIPs and BPs. At 150°C, the decrease in AA/Gly and the increase in UIPs and BPs occurred faster than at 110°C at a given molar ratio of AA/Gly. As expected, the molar ratio of AA/Gly also had significant influences on the consumption of AA/Gly, as did the effect of temperature.

When the molar ratio of AA/Gly was 4:1 with a reaction time of 10 - 240 min, the  $A_{294\text{ nm}}$  increased from 8.12 to 50.42, and the  $A_{420\text{ nm}}$  increased from 0.21 to 5.32 at 110°C. The concentrations of AA and Gly decreased from 24.26 to 22.95 mg/mL, and from

1.78 to 1.18 mg/mL, respectively (Figure 1A). Within the same reaction time and ratio of AA/Gly, the  $A_{294\text{ nm}}$  value ranged from 35.00 to 318.75, and the  $A_{420\text{ nm}}$  value ranged from 4.40 to 49.95 at 150°C. The concentrations of AA and Gly ranged from 22.04 to 7.99 mg/mL and from 1.29 to 0.35 mg/mL, respectively (Figure 2A). At a higher temperature of 150°C, as shown in Figure 2, when the reaction time was greater than 150 min, the curves of the decreasing concentration of AA/Gly and the increasing absorbance of UIPs and BPs became smoother. These

results suggested that a higher temperature was favourable for the consumption of AA/Gly and the formation of UIPs and BPs. When the molar ratio of AA/Gly was 1:4, the  $A_{294\text{ nm}}$  value ranged from 10.94 to 102.74, and the  $A_{420\text{ nm}}$  ranged from 1.65 to 14.28 at 150°C (Figure 2C). When the molar ratio of AA/Gly was 1:1, the  $A_{294\text{ nm}}$  value ranged from 13.55 to 88.99, and the  $A_{420\text{ nm}}$  value ranged from 1.51 to 11.26 at 150°C (Figure 2E). At both 110 and 150°C, the values of  $A_{294\text{ nm}}$  and  $A_{420\text{ nm}}$  with a molar AA/Gly ratio of 4:1 were much larger than those of

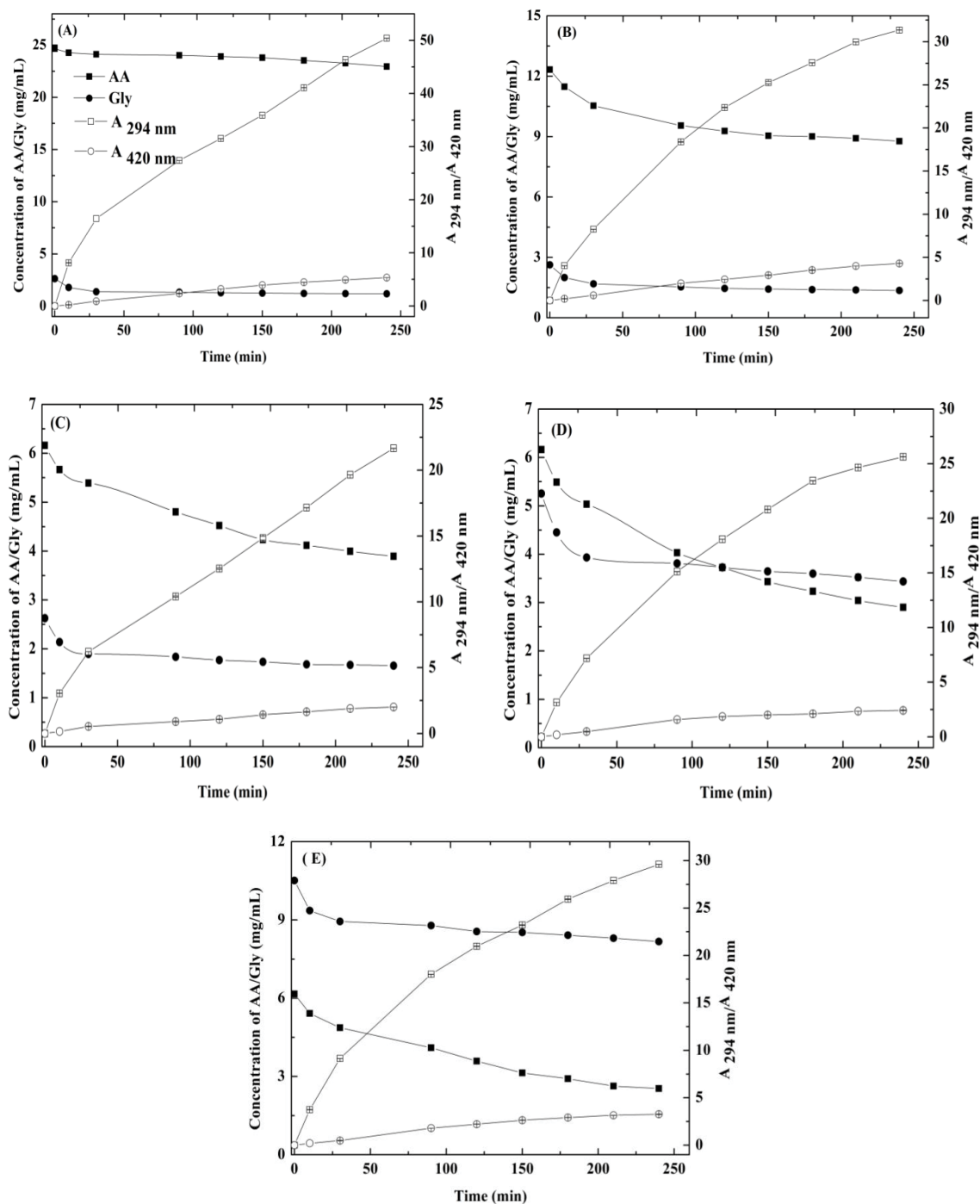


Figure 1. The effects of time on the degradation concentration of AA/Gly and absorbance values at 294 and 420 nm at 110°C (A = 4:1; B = 2:1; C = 1:4; D = 1:2; and E = 1:1).

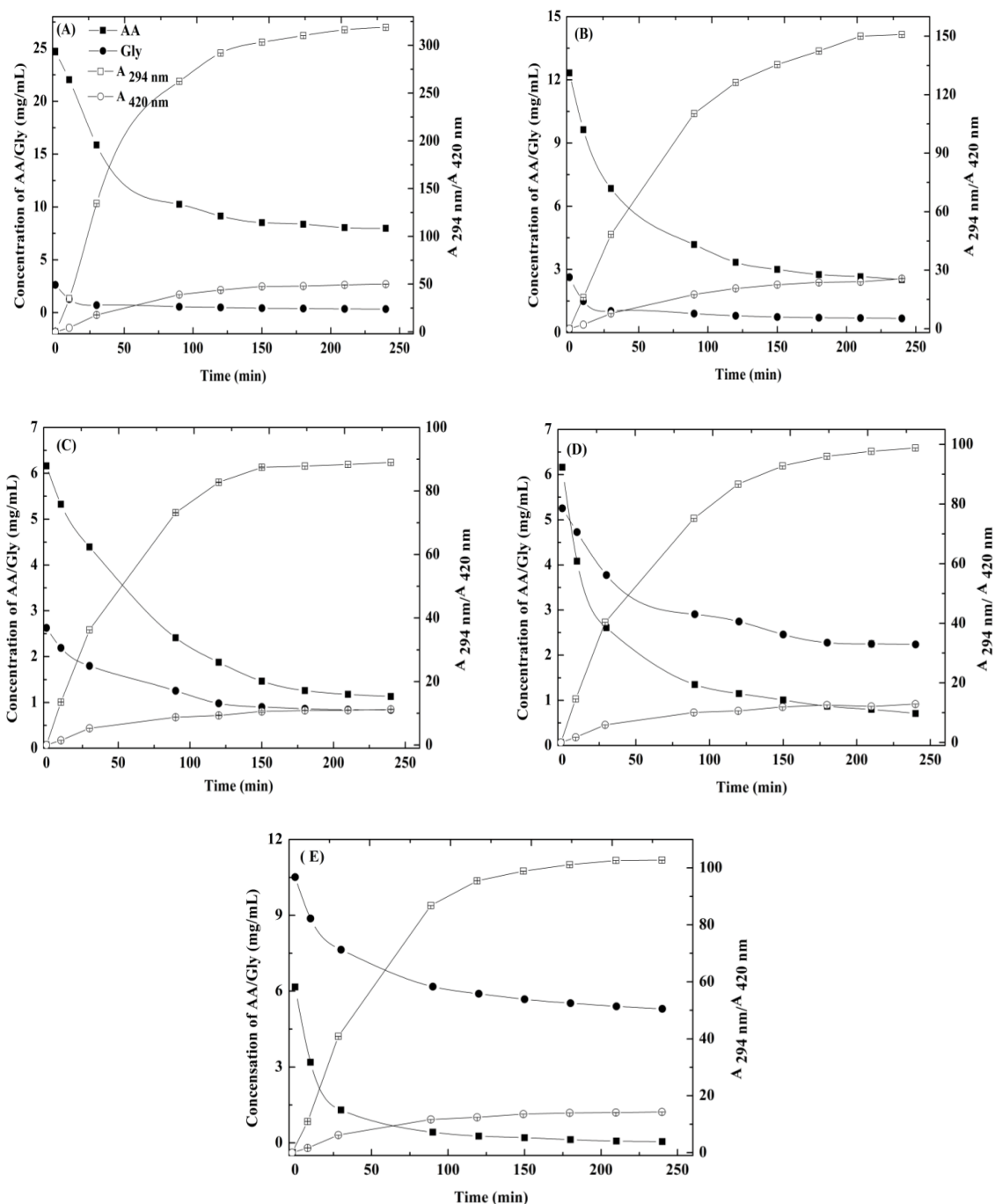


Figure 2. The effects of time on the degradation concentration of AA/Gly and absorbance values at 294 and 420 nm at 150°C (A = 4:1; B = 2:1; C = 1:4; D = 1:2; and E = 1:1).

other molar ratios. In terms of the consumption of AA/Gly and the formation of UIPs and BPs under different ratios of AA/Gly, this implied that the various ratios of AA/Gly had different effects on the formation of UIPs and BPs. When AA was excessive, it was more favourable for the formation of BPs. According to the change tendency of Gly/AA, as well as the tendency of the  $A_{294\text{ nm}}$  and  $A_{420\text{ nm}}$  values shown in Figures 1 and 2, it was found that the extent of the concentration in Gly was not as large as that of AA at experimental parameters (time, temperature, and ratio of AA/Gly). These results suggested that the decrease in the

concentration of Gly was not very large, which may be due to the better stability of Gly as compared to that of AA (Li *et al.*, 2016b; 2016c).

*The absorbance of BPs under different parameters*

The effects of the parameters on the absorbance at 420 nm are shown in Figure 3. The influences of temperature and the AA/Gly ratio on the absorbance at 420 nm were also dominant. At lower temperatures (110 and 120°C) and different ratios of AA/Gly, the absorbance at 420 nm increased with prolonged reaction time. However, at higher

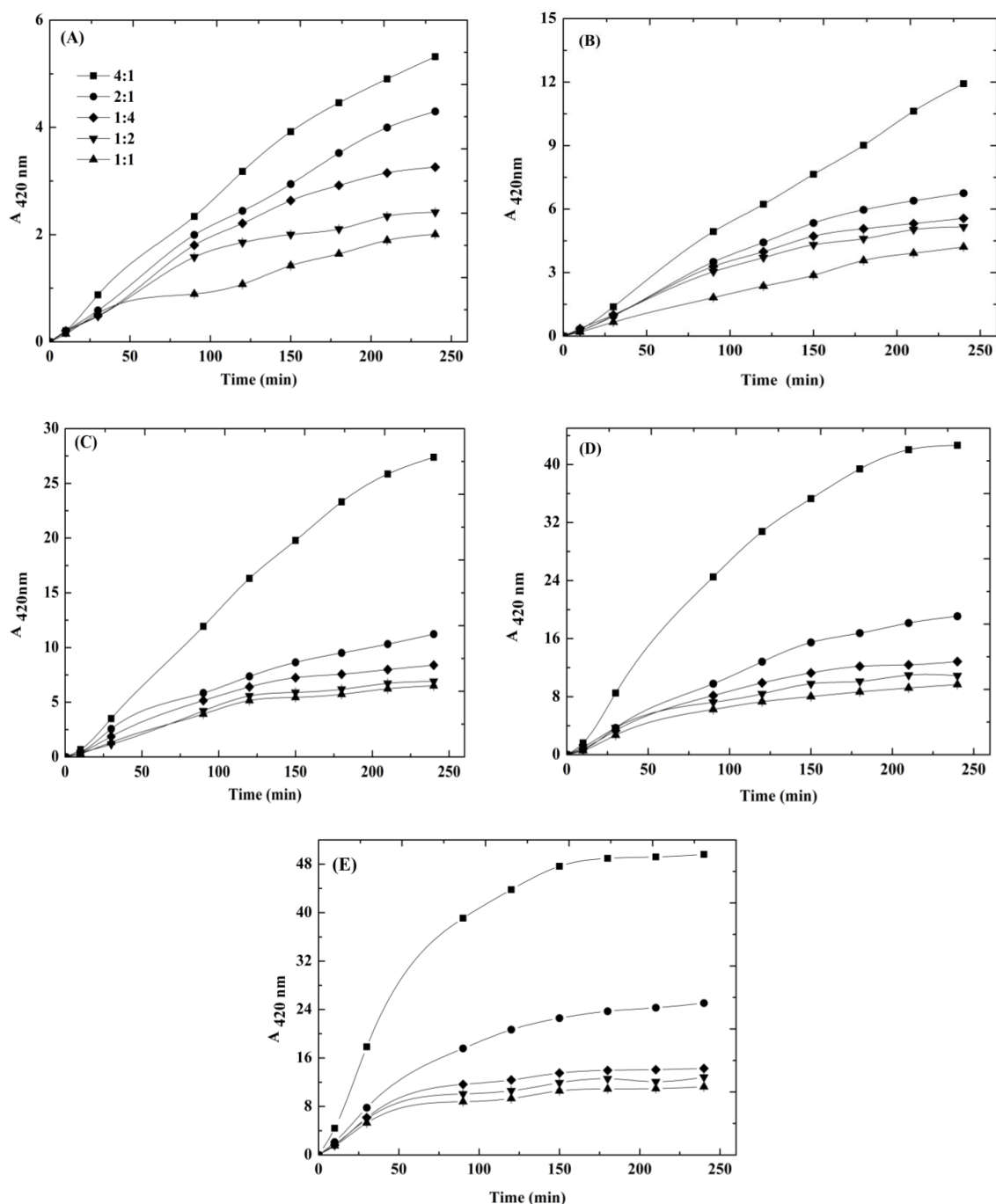


Figure 3. The effects of time on absorbance at 420 nm under different ratios of AA/Gly and reaction temperatures (A = 110°C; B = 120°C; C = 130°C; D = 140°C; and E = 150°C).

temperatures (140 and 150°C) and at the same AA/Gly ratio, the absorbance curve at 420 nm became smooth with a prolonged reaction time. The order of the influence of the AA/Gly ratio on the absorbance at 420 nm was 4:1, 2:1, 1:4, 1:2, and 1:1.

#### *The study of kinetics of the NEB reaction* *The formation schemes of BPs*

There were three major stages in the formation of BPs in NEB reaction including the early-stage products, intermediate products (IMDP), and final state products BPs. First, the decomposition or

degradation products came from the raw materials, which included some small volatile molecules and compounds such as aldehydes, ketones, and olefin alcohols (Benjakul *et al.*, 2005; Ajouz *et al.*, 2010; Yu *et al.*, 2012b; Li *et al.*, 2016b). Second, in the middle stage, the conjugate effects of the small compounds led to the absorption at 294 nm, and were named UIPs. Finally, BPs were formed after UIPs aggregated to a certain extent, which had an outstanding absorption at 420 nm (Brands *et al.*, 2000; Yu *et al.*, 2017). According to the analysis of the NEB reaction stages, the formation of BPs can be proposed simply as

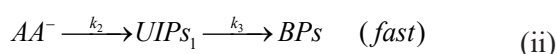
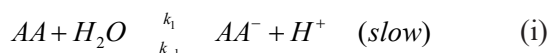
follows:



Regarding the formation of BPs, there were three major possible pathways: (1) the self-degradation or isomerisation of AA, (2) the reaction between  $IMDP_1$  coming from the self-degradation or isomerisation of AA and  $IMDP_2$  coming from the dissociation of Gly, and (3) the self-degradation of Gly.

In the process of self-degradation of AA, the first pathway would not be ignored (Li *et al.*, 2016a; 2016b; 2016c; Yu *et al.*, 2017), which would augment the absorbance value at 420 nm. However, a previous report (Li *et al.*, 2016a) showed that the solution had no absorption at 294 and 420 nm when the temperature was 150°C and the time was 240 min during the self-degradation process of Gly. Therefore, the third pathway for forming BPs which came from the self-degradation of Gly, could be negligible.

*In the absence of Gly*  
Scheme 1



On the basis of the mechanism of self-degradation or isomerisation of AA without air involved, the formation rate of BPs in the absence of Gly may be given as Eq. 2:

$$\frac{d[BPs]}{dt} = k_3[UIPS_1] = k_2[AA^-] \quad (Eq. 2)$$

By applying the steady state approximation rule with respect to  $[AA^-]$ , the formation rate of  $[AA^-]$  is given as Eq. 3:

$$\frac{d[AA^-]}{dt} = k_1[AA][H_2O] - k_{-1}[AA^-][H^+] - k_2[AA^-] \quad (Eq. 3)$$

Based on steady-state conditions, the expression for the concentration of  $AA^-$  would be gained, and substituting the expression for  $[AA^-]$  into Eq. 2, the rate of formation of BPs would be Eq. 4:

$$\frac{d[BPs]}{dt} = \frac{k_1 k_2 [AA][H_2O]}{k_{-1}[H^+] + k_2} \quad (Eq. 4)$$

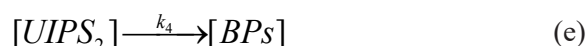
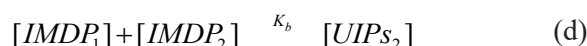
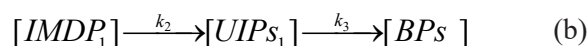
Since the concentration of hydrogen ions was small, and the amount of water was large, using a suitable approximation, the rate law in Eq. 4 was reduced to Eq. 5:

$$\frac{d[BPs]}{dt} = k_1[AA][H_2O] \approx k_1'[AA] \quad (Eq. 5)$$

The rate law in Eq. 5 suggested that the formation rate of BPs was a pseudo-first order dependence of rate with respect to AA in the absence of Gly (Li *et al.*, 2016a; 2016c). In the system in the absence of Gly, the formation rate of BPs was mainly due to the self-degradation of AA.

*In the presence of Gly*  
Scheme 2

Based on these experimental results and observations, the possible pathway of the NEB reaction of AA/Gly is proposed as follows in the reaction system between AA and Gly, as shown in Scheme 2.



According to Scheme 2, the formation rate of BPs is given by Eq. 6:

$$\frac{d[BPs]}{dt} = k_3[UIPS_1] + k_4[UIPS_2] \quad (Eq. 6)$$

Based on steady-state conditions, the rate of BPs formation may also be given as Eq. 7:

$$\frac{d[BPs]}{dt} = k_2[IMDP_1] + k_4[UIPS_2] \quad (Eq. 7)$$

The concentration of  $IMDP_1$  is obtained with respect to formulas (a) and (b) based on the steady-state conditions, and  $[IMDP_1]$  was given as Eq. 8:

$$[IMDP_1] = \frac{k_1}{k_2} [AA] \quad (Eq. 8)$$

Considering the reversible reaction of formula (c), the concentration of  $IMDP_2$  can be obtained by Eq. 9:

$$[IMDP_2] = k_a [Gly] \quad (Eq. 9)$$

Combining formulas (d) and (e) by applying steady-state conditions, Eq. 10 was obtained:

$$K_b[IMDP_1][IMDP_2] = k_4[UIPS_2] \quad (\text{Eq. 10})$$

Substituting  $[IMDP_1]$  and  $[IMDP_2]$  from Eq. 8 and Eq. 9 into Eq. 10, Eq. 11 was obtained:

$$k_4[UIPS_2] = \frac{k_1 K_a K_b}{k_2} [AA][Gly] \quad (\text{Eq. 11})$$

By substituting Eq. 8 and Eq. 11 into Eq. 7, Eq. 12 for the formation of BPs was obtained:

$$\frac{d[BP_s]}{dt} = k_1 \left\{ 1 + \frac{K_a K_b}{k_2} [Gly] \right\} [AA] \quad (\text{Eq. 12})$$

The concentration of Gly residue in solution significantly dropped, as shown Figures 1 and 2, and the concentration of Gly was low. Eq. 8 and Eq. 9 were reversible reaction so that  $K_a$  and  $K_b$  were not much greater than  $k_2$ , and using a suitable approximation of  $K_a K_b [Gly] / k_2 \ll 1$ , Eq. 12 can be simplified to Eq. 13.

$$\frac{d[BP_s]}{dt} = k_1 [AA] \quad (\text{Eq. 13})$$

Combining Eq. 13 and Eq. 1, we conjectured that  $\alpha$  was 1 and  $\beta$  was zero, and thus Eq. 1 would be reduced to:

$$\frac{dC_{BP_s}}{dt} = k' C_{AA} \quad (\text{Eq. 14})$$

Based on these results, in the system in the absence or presence of Gly, Eq. 5, 13, and 14 indicated that the formation rate of BPs depended only on the consumption of AA, which followed the pseudo-first order reaction kinetic characteristics mainly based on the decreasing concentration of AA. In the system in the presence of Gly, although the residual

concentration of Gly was not negligible under various reaction conditions, the concentration of Gly did not significantly change due to its stability. In other words, for the generation of BPs, the influence of Gly was small, which combined with the reaction coefficient  $k$  into a constant  $k'$  in terms of formula (a). According to the pseudo-first order reaction model, the formation rate of BPs would be presented as Eq. 14. The formation rate constant of BPs and  $\alpha$  as a function of heating time, and the correlation coefficient ( $R^2$ ) are summarised in Table 2 when the investigated temperature ranged from 110 to 150°C. The increasing absorbance of BPs was presented as the absorption at 420 nm.

The fitting versus  $1/T$  under different ratios of AA/Gly was studied based on the pseudo-first order, which depended on consumption of AA. The activation energy ( $E_a$ ) was estimated on the basis of the Arrhenius relationship, and was described in Eq. 15.

$$\ln(k') = -\frac{E_a}{RT} + A \quad (\text{Eq. 15})$$

Based on the fitting of versus  $1/T$ , the lowest value of  $E_a$  was approximately 60.76 kJ.mol<sup>-1</sup> when the AA/Gly ratio was 4:1. When the AA/Gly ratio was 1:1, the  $E_a$  was the largest, approximately 88.84 kJ.mol<sup>-1</sup>. When the ratio of AA/Gly was 1:4, the  $E_a$  for the formation of BPs was 70.16 kJ.mol<sup>-1</sup>. In the absence of Gly, the  $E_a$  was approximately 58.06 kJ.mol<sup>-1</sup>. These results suggested that when Gly was in excess, the formation  $E_a$  for BPs was slightly higher than for when there was an excess of AA. It was confirmed that the higher molar concentration of AA had a remarkable influence on the formation of BPs. Although the excess Gly also contributed to the formation of BPs, that contribution was not large.

Table 2. The formation rate of  $A_{420 \text{ nm}}$  at different temperatures and ratios of AA/Gly.

Temperature (°C)	Absence of Gly $k' (R^2)^a$	4:1 $k' (R^2)$	2:1 $k' (R^2)$	1:1 $k' (R^2)$	1:2 $k' (R^2)$	1:4 $k' (R^2)$
110	0.0122 (0.9854)	0.0522 (0.9930)	0.0182 (0.9992)	0.0043 (0.9942)	0.0098 (0.9973)	0.0140 (0.9950)
120	0.0220 (0.9411)	0.0680 (0.9972)	0.0293 (0.9947)	0.0098 (0.9905)	0.0161 (0.9944)	0.0233 (0.9903)
130	0.0318 (0.9645)	0.1207 (0.9926)	0.0455 (0.9983)	0.0199 (0.9949)	0.0292 (0.9940)	0.0344 (0.9978)
140	0.0487 (0.9491)	0.1828 (0.9979)	0.0811 (0.9917)	0.0378 (0.9905)	0.0418 (0.9982)	0.0701 (0.9961)
150	0.0705 (0.8513)	0.3056 (0.9941)	0.1461 (0.9997)	0.0593 (0.9911)	0.0910 (0.9987)	0.1096 (0.9951)
$E_a$ (kJ/mol)	58.06 ± 2.29	60.76 ± 4.23	69.67 ± 3.69	88.84 ± 4.12	72.70 ± 5.08	70.16 ± 4.07

<sup>a</sup>Li et al. (2016c), the concentration of AA was 0.5 mmol.

## Conclusion

In the present work, the formation kinetic behaviour of BPs was investigated with different parameters including temperature, time, and ratio of AA/Gly. Results showed that the excess ratio of AA had a remarkable effect on the formation of BPs. Based on the rate constant and the  $E_a$ , it could be concluded that BPs were formed by the self-degradation of AA and the reaction of AA and Gly. The formation of BPs was pseudo-first order based on the possible reaction scheme. Based on the assumption of a kinetic mathematical model and the possible pathway, the formation of BPs followed the pseudo-first order, and the  $E_a$  was 60.76 and 70.16 kJ/mol at AA/Gly ratios of 4:1 and 1:4, respectively.

## Acknowledgement

The authors acknowledge the financial support received from the National Natural Science Foundation of China (project no.: 31960512), the Natural Science Foundation of Hubei Province, China (project no.: 2018CFB650), the Beijing Key Laboratory of Flavour Chemistry, Beijing Technology and Business University (project no.: SPFW-2017-YB04), and the Incubation Project for High-level Scientific Research Achievements of Hubei Minzu University, China (project no.: 4205012).

## References

- Ahrné, L., Andersson, C. G., Floberg, P., Rosen, J. and Lingnert, H. 2007. Effect of crust temperature and water content on acrylamide formation during baking of white bread: steam and falling temperature baking. *LWT - Food Science and Technology* 40(10): 1708-1715.
- Ajouz, E. H., Leopold, T., Dalle, O. F. and Benajiba, A. 2010. Effects of pH on caramelization and Maillard reaction kinetics in fructose-lysine model systems. *Journal of Food Science* 66(7): 926-931.
- Benjakul, W., Lertittikul, W. and Bauer, F. 2005. Antioxidant activity of Maillard reaction products from a porcine plasma protein-sugar model system. *Food Chemistry* 93(2): 189-196.
- Bhore, N. A., Klein, M. T. and Bischoff, K. B. 1990. The delplot technique: a new method for reaction pathway analysis. *Industrial and Engineering Chemistry Research* 29(2): 313-316.
- Boekel, M. A. J. S. V. 1998. Effect of heating on Maillard reactions in milk. *Food Chemistry* 62(4): 403-414.
- Brands, C. M. J., Alink, G. M., Boekel, M. A. and Jongen, W. M. 2000. Mutagenicity of heated sugar-casein systems: effect of the Maillard reaction. *Journal of Agricultural and Food Chemistry* 48(6): 2271-2275.
- Gabriel, A. A., Cayabyab, J. E. C., Tan, A. K., Corook, M. L. F. and Ables, E. J. O. 2015. Development and validation of a predictive model for the influences of selected product and process variables on ascorbic acid degradation in simulated fruit juice. *Food Chemistry* 177: 295-303.
- Hodge, J. E. 1953. Dehydrated foods: chemistry of browning reactions in model systems. *Journal of Agricultural and Food Chemistry* 1: 625-651.
- Isleroglu, H., Kemerli, T., Sakin-Yilmazer, M., Guven, G. and Ozdestan, O. 2012. Effect of steam baking on acrylamide formation and browning kinetics of cookies. *Journal of Food Science* 77(10): 257-263.
- Kambo, N. and Upadhyay, S. K. 2012. Kinetic behaviour of ascorbic acid-fructose browning reaction in alkaline medium. *Indian Journal of Chemical Technology* 19(2): 128-133.
- Leong, L. P. and Wedzicha, B. L. 2000. A critical appraisal of the kinetic model for the Maillard browning of glucose with glycine. *Food Chemistry* 68(1): 21-28.
- Lerici, C. R., Barbanti D., Manzano, M. and Cherubin. S. 1990. Early indicators of chemical changes in foods due to enzymic or non enzymic browning reactions. 1: study on heat treated model systems. *Lebensmittel-Wissenschaft und Technology* 23: 289-294.
- Lertittikul, W., Benjakul, S. and Tanaka, M. 2007. Characteristics and antioxidative activity of Maillard reaction products from a porcine plasma protein-glucose model system as influenced by pH. *Food Chemistry* 100(2): 669-677.
- Li, Y., Yang, Y. and Yu, A. N. 2016b. The research of volatiles compounds from the Maillard reaction of L-ascorbic acid and glycine. *International Journal of Food Science and Technology* 51(6): 1349-1359.
- Li, Y., Yang, Y., Yu, A. N. and Hu, T. W. 2016c. The process and dynamic research for the non-enzymatic browning reaction about the self-degradation of L-ascorbic acid. *Science and Technology of Food Industry* 37(4): 117-122.
- Li, Y., Yang, Y., Yu, A. N. and Wang, K. 2016a. Effects of reaction parameters on self-degradation of L-ascorbic acid and self-degradation kinetics. *Food Science and Biotechnology*

- 25(1): 97-104.
- Maillard, L. C. 1912. Action of amino acids on lessons: formation of melanoidins systematically. *Comptes Rendus de l'Académie des Sciences* 154: 66-68.
- Martins, S. I. F. S. and Boekel, M. A. J. S. V. 2005a. Kinetics of the glucose/glycine Maillard reaction pathways: influences of pH and reactant initial concentrations. *Food Chemistry* 92(3): 437-448.
- Martins, S. I. F. S. and Boekel, M. A. J. S. V. 2005b. A kinetic model for the glucose/glycine Maillard reaction pathways. *Food Chemistry* 90(1-2): 257-269.
- Martins, S. I. F. S., Jongen, W. M. F. and Boekel, M. A. J. S. V. 2000. A review of Maillard reaction in food and implications to kinetic modelling. *Trends in Food Science and Technology* 11(9-10): 364-373.
- Mitra, J., Shrivastava, S. L. and Rao, P. S. 2015. Non-enzymatic browning and flavour kinetics of vacuum dried onion slices. *International Agrophysics* 29(1): 91-100.
- Montano, A., Casado, F. J., Rejano, L., Sanchez, A. H. and Castro, A. D. 2006. Degradation kinetics of the antioxidant additive ascorbic acid in packed table olives during storage at different temperatures. *Journal of Agricultural and Food Chemistry* 54(6): 2206-2210.
- Mundt, S. and Wedzicha, B. L. 2003. A kinetic model for the glucose-fructose-glycine browning reaction. *Journal of Agricultural and Food Chemistry* 51(12): 3651-3655.
- Rogacheva, S. M., Kuncheva, M. J., Panchev, I. and Obretenov, T. D. 1995. L-ascorbic acid in nonenzymatic reactions. I. Reaction with glycine. *European Food Research and Technology* 200(1): 52-58.
- Sapei, L. and Hwa, L. 2014. Study on the kinetics of vitamin C degradation in fresh strawberry juice. *Procedia Chemistry* 9: 62-68.
- Serpen, A. and Gokmen, V. 2007. Reversible degradation kinetics of ascorbic acid under reducing and oxidizing conditions. *Food Chemistry* 104(2): 721-725.
- Shallenberger, R. S., Smith, O. and Treadway, R. H. 1959. Food color change, role of the sugars in the browning reaction in potato chips. *Journal of Agricultural and Food Chemistry* 7(4): 274-277.
- Stadler, R. H., Blank, I., Varga, N., Robert, F. and Hau, J. 2002. Food chemistry - acrylamide from Maillard reaction products. *Nature* 419: 449-450.
- Tang, L. P., Zhou, Y. Y. and Yu, A. N. 2014. Comparison of UV spectrophotometry and HPLC in determination of ascorbic acid in Maillard reaction. *Science and Technology of Food Industry* 35(10): 79-82.
- Tiwari, B. K., Donnell, C. P. O., Muthukumarappan, K. and Cullen, P. J. 2009. Ascorbic acid degradation kinetics of sonicated orange juice during storage and comparison with thermally pasteurized juice. *LWT - Food Science and Technology* 42(3): 700-704.
- Vernin, G., Chakib, S., Rogacheva, S. M., Obreenov, T. D. and Parkanyi, C. 1997. Thermal decomposition of ascorbic acid. *Carbohydrate Research* 305(1): 1-15.
- Wedzicha, B. L. and Mcweeny D. J. 1974. Non-enzymic browning reactions of ascorbic acid and their inhibition. The identification of 3-deoxy-4-sulphopentosulose in dehydrated, sulphited cabbage after storage. *Journal of the Science of Food and Agriculture* 25(5): 577-587.
- Yu, A. N., Tan, Z. W. and Wang, F. S. 2012b. Mechanism of formation of sulphur aroma compounds from L-ascorbic acid and L-cysteine during the Maillard reaction. *Food Chemistry* 132(3): 316-323.
- Yu, A. N., Zhou, Y. Y. and Yang, Y. N. 2017. Kinetics of browning and correlations between browning degree and pyrazine compounds in L-ascorbic acid/acidic amino acid model systems. *Food Chemistry* 221: 678-684.
- Yu, X. Y., Zhao, M. Y., Hu, J., Zeng, S. T. and Bai, X. L. 2012a. Correspondence analysis of antioxidant activity and UV-Vis absorbance of Maillard reaction products as related to reactants. *LWT - Food Science and Technology* 46(1): 1-9.
- Zhou, Y. Y., Li, Y. and Yu, A. N. 2015. Optimum extraction conditions for pyrazine compounds from Maillard reaction mixture by headspace solid-phase microextraction. *Food Science* 36(6): 119-123.
- Zhou, Y. Y., Li, Y. and Yu, A. N. 2016. The effects of reactants ratios, reaction temperatures and times on Maillard reaction products of the L-ascorbic acid/L-glutamic acid system. *Food Science and Technology* 36(2): 68-74.